

Supporting information

Morphogenesis of biofilms in porous media and control on hydrodynamics

Dorothee L. Kurz^{1,2}, Eleonora Secchi^{1*}, Roman Stocker¹, Joaquin Jimenez-Martinez^{1,2*}

(1) Institute of Environmental Engineering, Department of Civil, Environmental and Geomatic Engineering, ETH Zurich, Laura-Hezner-Weg 7, 8093 Zurich, Switzerland

(2) Department Water Resources and Drinking Water, Eawag, Swiss Federal Institute of Aquatic Science and Technology, 8600 Dübendorf, Switzerland

*To whom correspondence may be addressed: esecchi@ethz.ch; joaquin.jimenez@eawag.ch

Content:

Number of pages: 9

Figures S1-S7

Tables S1-S3

Details on the assumption of inverse proportionality of concentration and porosity used in the Main Manuscript to derive the relationship between image intensity and permeability.

With the concentration of the biofilm, c being the ratio of the biofilm mass M_b and the total volume V_t :

$$c = \frac{M_b}{V_t} \quad \text{Eq. S1}$$

And the density of the biofilm ρ being the ratio of the biofilm mass M_b and the biofilm volume V_b :

$$\rho = \frac{M_b}{V_b} \quad \text{Eq. S2}$$

When combining equations Eq. S1 and Eq. S2 by replacing M_b , we obtain:

$$c \cdot V_t = \rho \cdot V_b \quad \text{Eq. S3}$$

With the porosity of the biofilm n_b being the ratio of the void volume in the biofilm $V_{b,void}$ and the biofilm volume V_b :

$$n_b = \frac{V_{b,void}}{V_b} \quad \text{Eq. S4}$$

We can now replace V_b in Eq. S3 with Eq. S4 and obtain a simplified inverse proportionality between the concentration and the porosity.

$$c \cdot V_t = \rho \cdot \frac{V_{b,void}}{n_b} \rightarrow c \sim \frac{1}{n_b} \quad \text{Eq. S5}$$

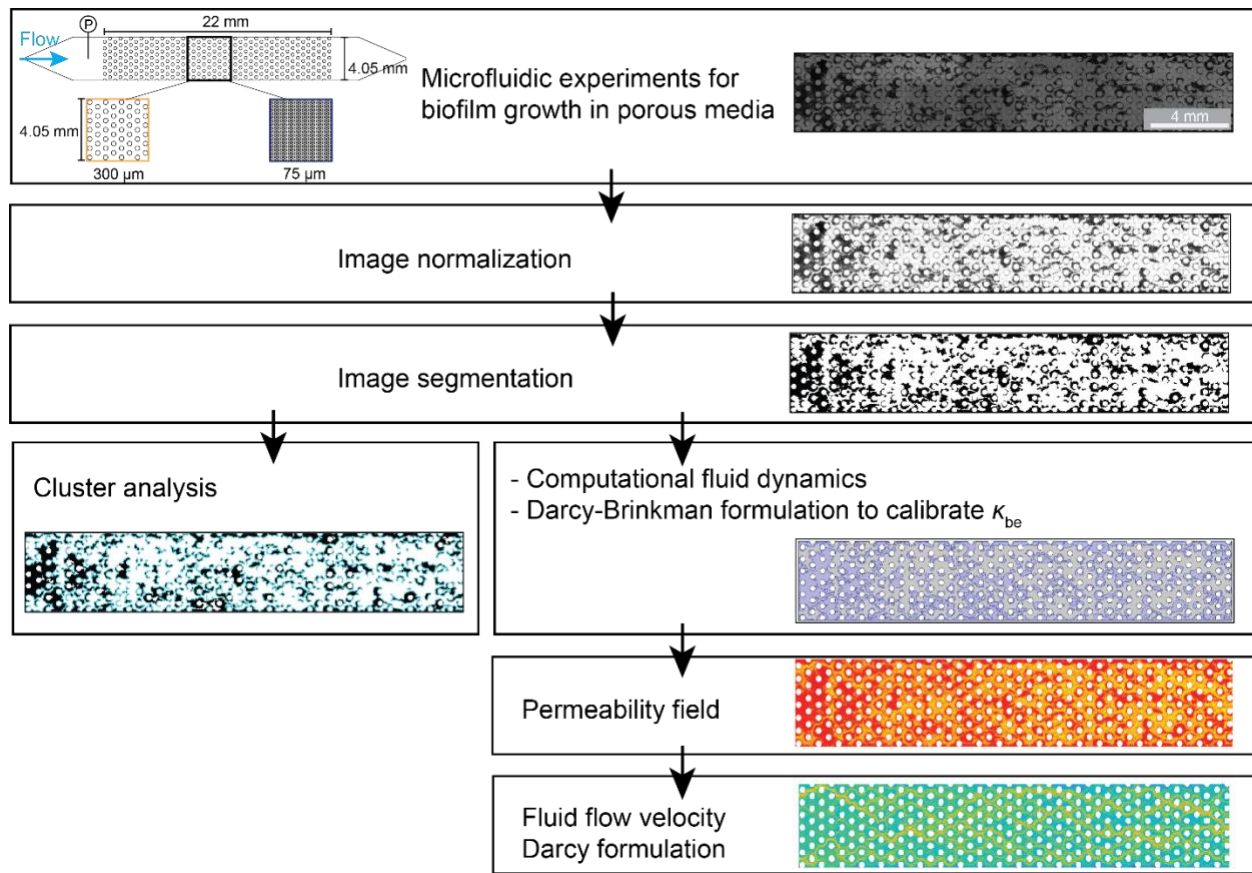


Figure S1: Overview of the methods used to analyze the cluster dynamics and to obtain spatially resolved permeability and velocity field of the biofilm–porous medium system. Details for every step can be found in the Main Manuscript. After running microfluidic experiments of biofilm growth within porous media with time-lapse imaging, the images were normalized and segmented for cluster analysis. Segmented images were also used to obtain the effective permeability of the biofilm from computational fluid dynamics modelling using a Darcy–Brinkman formulation. The model resolved flow through the biofilm matrix as a continuum (Darcy’s law) and through the open paths by Navier–Stokes flow. The effective permeability of the biofilm (shown in lilac) was calibrated against experimental pressure measurements. The effective permeability of the biofilm together with a model derived from a method used in light transmission micro-tomography were used to obtain the biofilm–porous medium permeability field. The permeability fields were then used to obtain the flow through the entire biofilm–porous medium system by using Darcy’s law. The resulting permeability fields were validated against experimental pressure measurements.

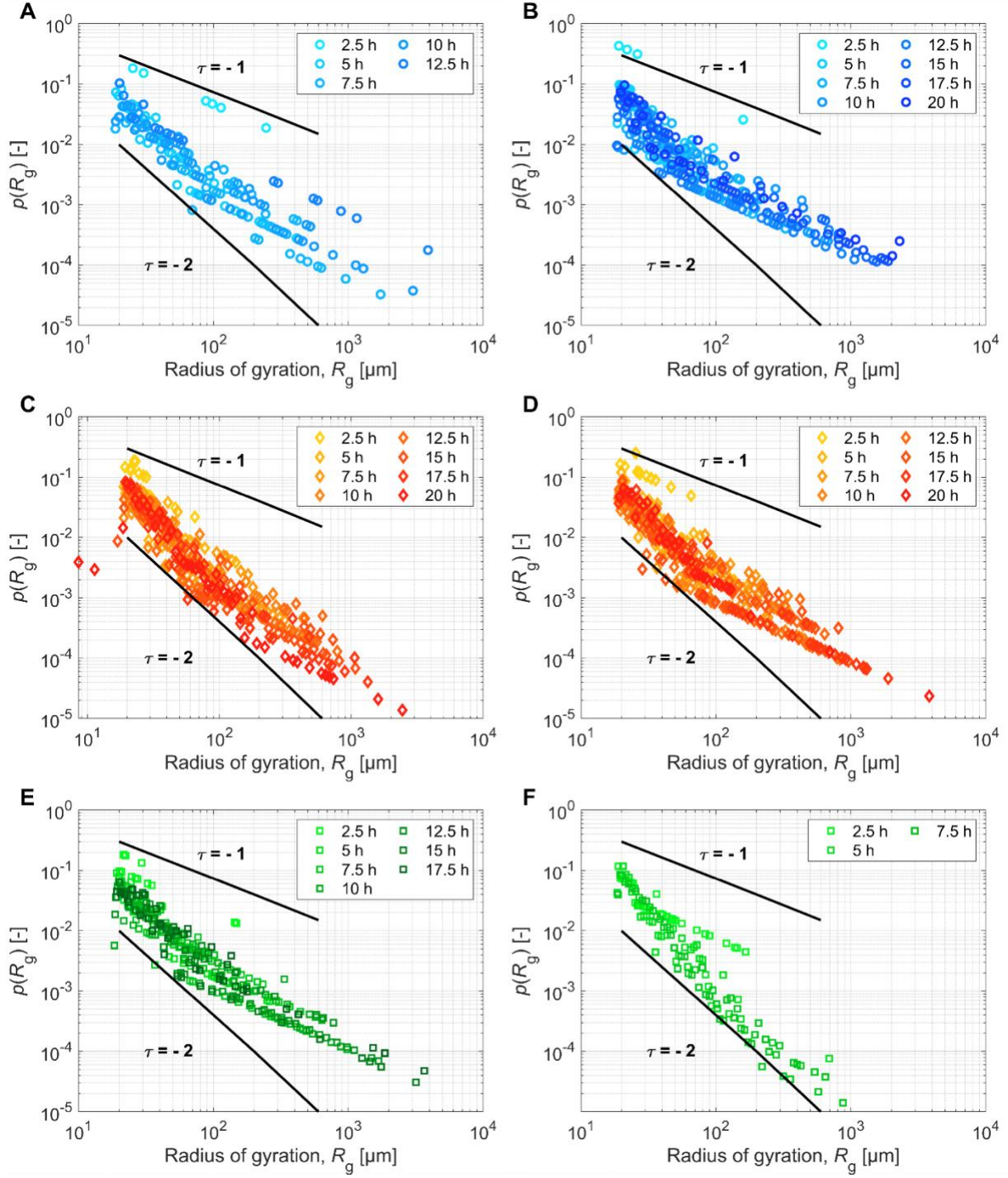


Figure S2: Probability density functions of the radius of gyration R_g , the radius of a circle of the same area as the biofilm cluster, at different time points (colour coded) for the replicates of the different experimental conditions shown in Figure 3 in the Main Manuscript at (A/B) $d = 300 \mu\text{m}$ and $Q = 1 \text{ mL/h}$, (C/D) $d = 300 \mu\text{m}$ and $Q = 0.2 \text{ mL/h}$, and (E/F) $d = 75 \mu\text{m}$ and $Q = 1 \text{ mL/h}$.

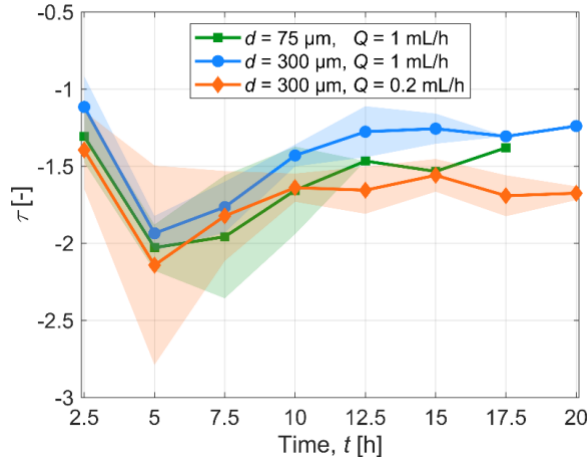


Figure S3: Temporal evolution of the spectrum slope τ fitted by linear least-square regression to the probability density function of the radius of gyration $p(R_g)$ (Main Manuscript Fig.3 and Fig. S2) for the experimental conditions $d = 75 \mu\text{m}$ and $Q = 1 \text{ mL/h}$ (green squares), $d = 300 \mu\text{m}$ and $Q = 1 \text{ mL/h}$ (blue circles) and $d = 300 \mu\text{m}$ and $Q = 0.2 \text{ mL/h}$ (orange diamonds). The shaded area indicates the standard deviation of the mean. For some replicates, the time point of percolation occurred at earlier times, therefore some data points at later time points do not have a shaded area.

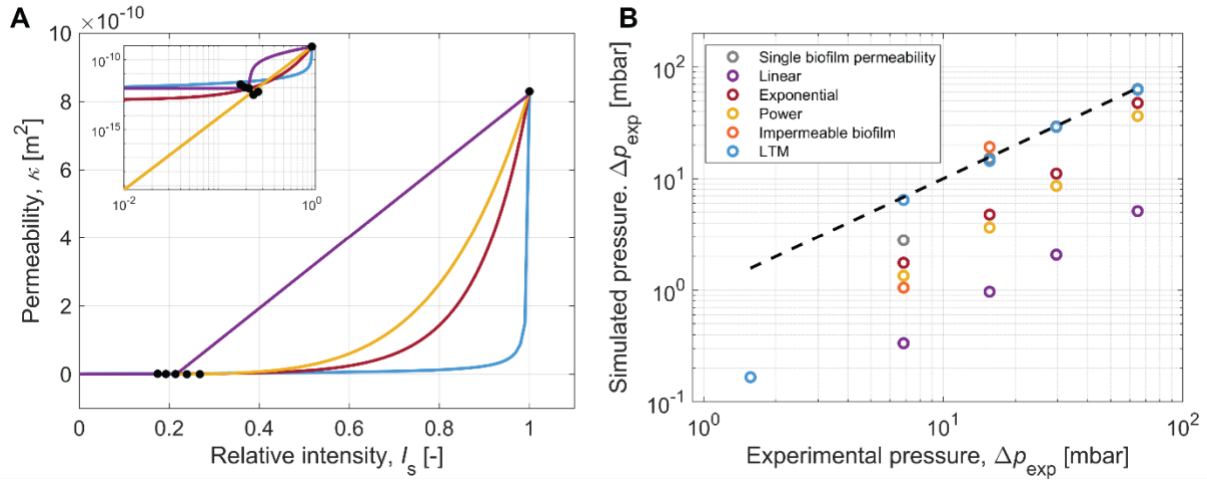


Figure S4: Fitting of alternative functions shown in Table S2 to relate relative image intensity to the permeability. (A) Alternative functions to relate the relative intensity of the experimental images of the biofilm to the effective permeability of the biofilm (Table S2), fitted to the data for the experimental conditions pore size $d = 300 \mu\text{m}$ and flow rate $Q = 1 \text{ mL/h}$. The inset is showing the same data on logarithmic scale (purple: linear function, yellow: power function; red: exponential function; blue: adapted function used in light tomography – LTM, see Main Manuscript for details and derivation). (B) Comparison of the simulated and experimentally obtained values of pressure difference across the porous medium to evaluate the performance of the functions shown in (A) for the created heterogeneous permeability field. Additionally, simulations were run for single effective permeability values of the biofilm (κ_{be}) as well as impermeable biofilms.

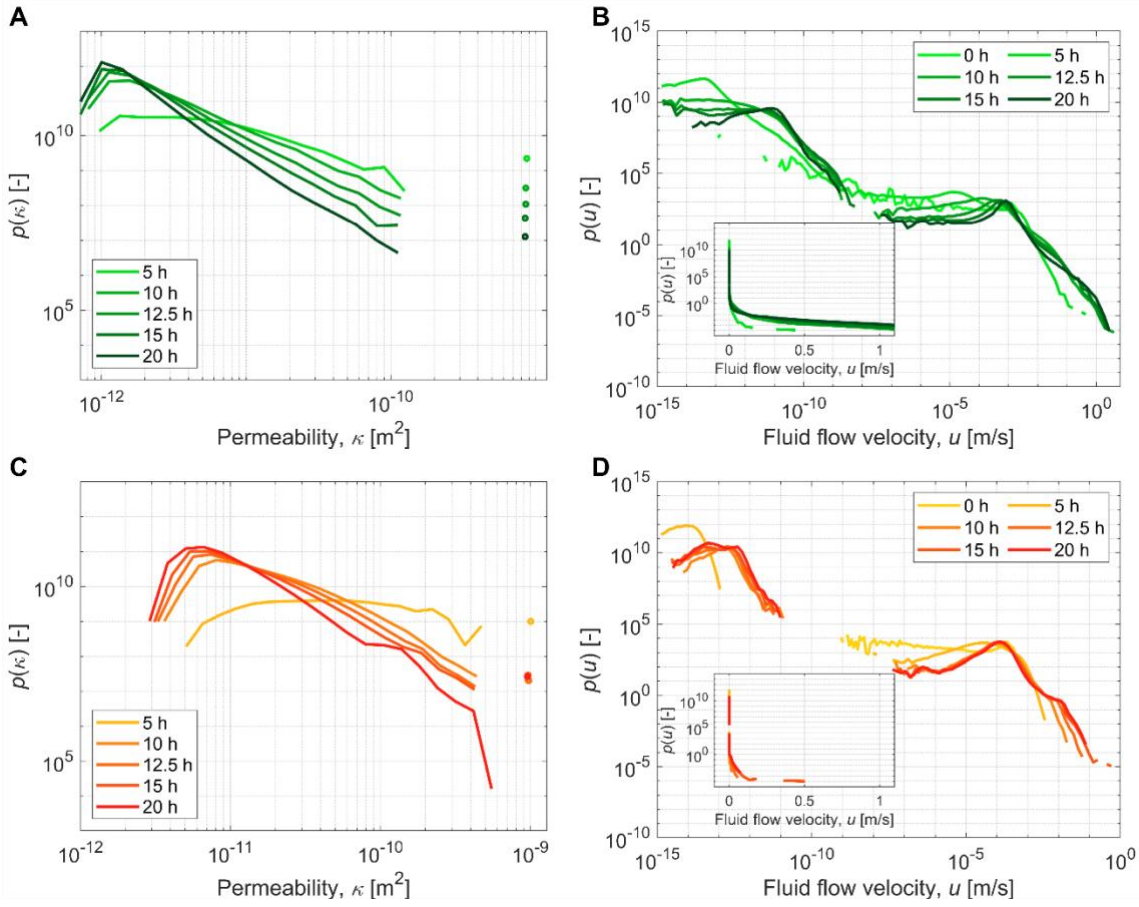


Figure S5: (A) Probability density functions of permeability $p(\kappa)$ for the biofilm-porous medium system $d = 75 \mu\text{m}$ and $Q = 1 \text{ mL/h}$ at five selected time points. The colour gradient indicates the temporal evolution for all panels. (B) Probability density functions of velocity $p(u)$ for the biofilm-porous medium system $d = 75 \mu\text{m}$ and $Q = 1 \text{ mL/h}$ at five selected time points. The inset shows the same data on a semi-logarithmic scale highlighting the high velocities. (C) Probability density functions of permeability $p(\kappa)$ for the biofilm-porous medium system $d = 300 \mu\text{m}$ and $Q = 0.2 \text{ mL/h}$ at five selected time points. (D) Probability density functions of velocity $p(u)$ for the biofilm-porous medium system $d = 300 \mu\text{m}$ and $Q = 0.2 \text{ mL/h}$ at five selected time points. The inset shows the same data on a semi-logarithmic scale highlighting the high velocities.

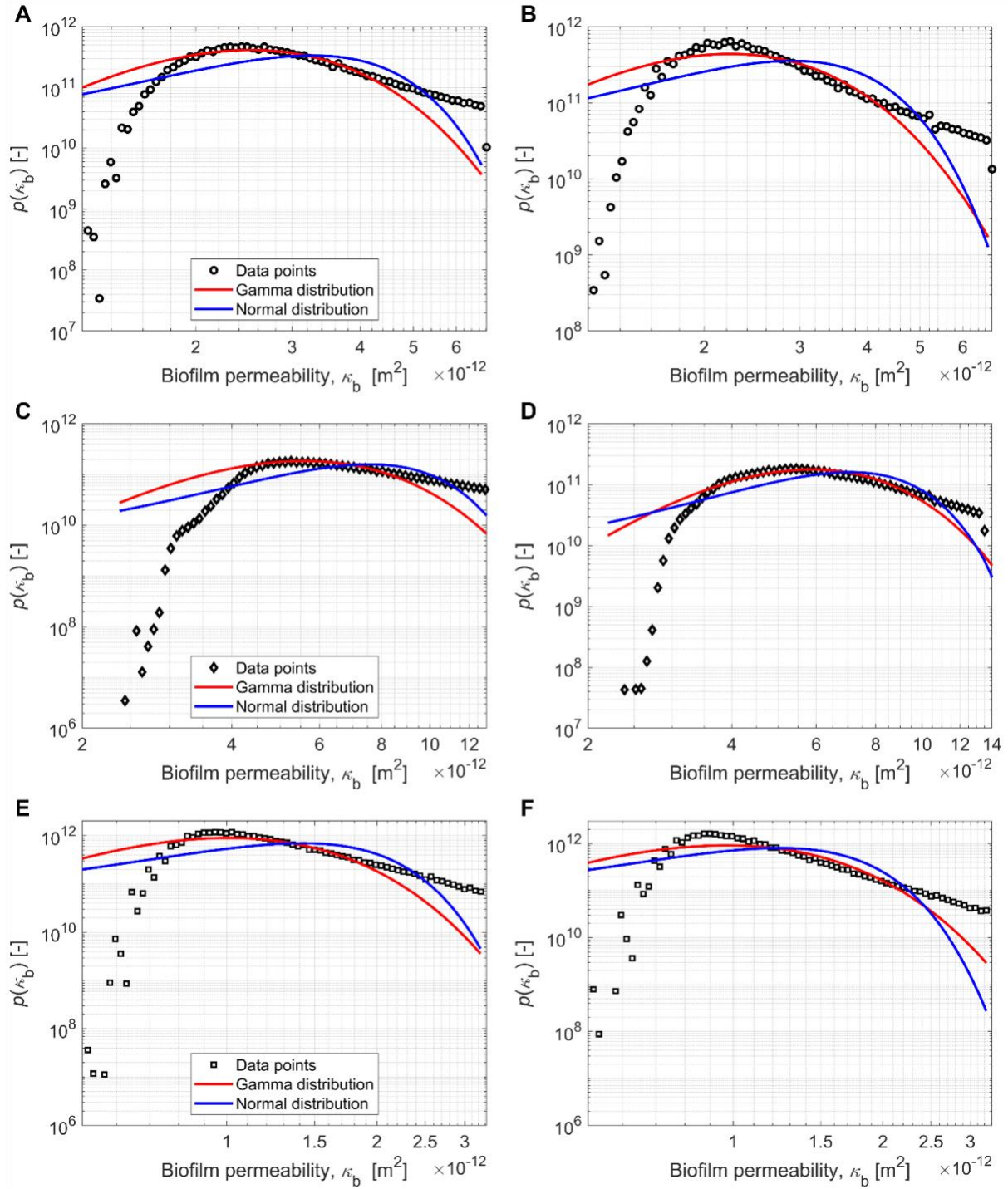


Figure S6: Probability density functions of the biofilm permeability κ_b (black symbols). The manually fitted Gamma distribution (red line) and the fitted Normal distribution (blue line) at (A) $t = 15$ h, $d = 300$ μm , $Q = 1$ mL/h, (B) $t = 20$ h, $d = 300$ μm , $Q = 1$ mL/h, (C) $t = 15$ h, $d = 300$ μm , $Q = 0.2$ mL/h, (D) $t = 20$ h, $d = 300$ μm , $Q = 0.2$ mL/h, (E) $t = 15$ h, $d = 75$ μm , $Q = 1$ mL/h, and (F) $t = 20$ h, $d = 75$ μm , $Q = 1$ mL/h.

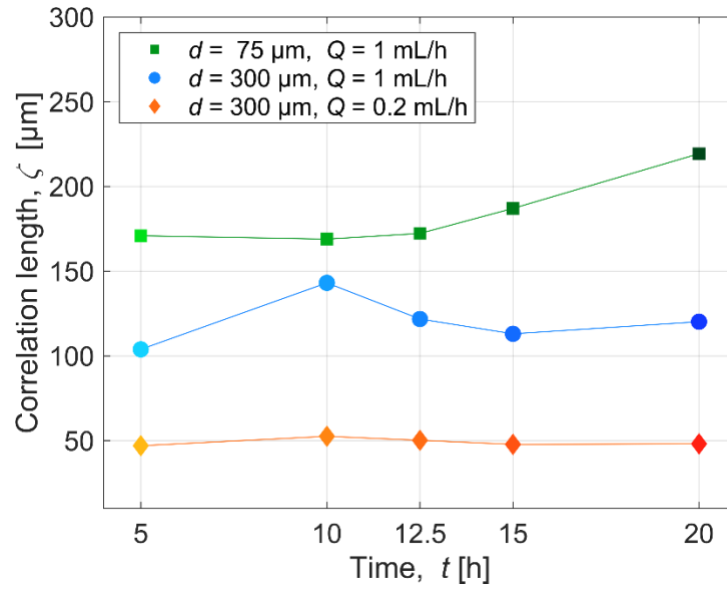


Figure S7: Omnidirectional correlation length ζ of permeability for the three experimental conditions and selected time points (greenish squares: $d = 75 \mu\text{m}$, $Q = 1 \text{ mL/h}$; blueish circles: $d = 300 \mu\text{m}$, $Q = 1 \text{ mL/h}$; and orangish diamonds: $d = 300 \mu\text{m}$, $Q = 0.2 \text{ mL/h}$). The colour gradients indicate the temporal evolution.

Table S1: Geometric mean of the image intensity of the biofilm I_s and the effective biofilm permeability κ_{be} for different time points used for calibration of the model adapted from light tomography model

$d = 300 \mu\text{m}, Q = 1 \text{ mL/h}$		
Time, t [h]	Geometric mean of I_s [-]	κ_{be} [m^2]
12.5	0.2679	$5.00 \cdot 10^{-13}$
15	0.2392	$3.00 \cdot 10^{-13}$
17.5	0.2139	$8.75 \cdot 10^{-13}$
20	0.1925	$1.05 \cdot 10^{-12}$
22.5	0.1743	$1.65 \cdot 10^{-12}$

$d = 75 \mu\text{m}, Q = 1 \text{ mL/h}$		
Time, t [h]	Geometric mean of I_s [-]	κ_{be} [m^2]
5	0.3398	$5.00 \cdot 10^{-13}$
10	0.2600	$1.25 \cdot 10^{-12}$
12.5	0.2214	$1.50 \cdot 10^{-12}$
15	0.1888	$1.42 \cdot 10^{-12}$
20	0.1476	$1.03 \cdot 10^{-12}$

$d = 300 \mu\text{m}, Q = 0.2 \text{ mL/h}$		
Time, t [h]	Geometric mean of I_s [-]	κ_{be} [m^2]
10	0.3830	$2.00 \cdot 10^{-12}$
12.5	0.3363	$1.15 \cdot 10^{-11}$
15	0.3048	$9.00 \cdot 10^{-12}$
17.5	0.2838	$1.10 \cdot 10^{-11}$
20	0.2699	$8.00 \cdot 10^{-12}$

Table S2: Functions linking permeability κ and relative image intensity I_s used to convert the biofilm-porous medium images to permeability fields. Details can be found in the Main Manuscript. I_m is the mean intensity measured within the biofilm.

Linear	Exponential	Power
$\kappa = \begin{cases} \text{const.}, & I_s < I_m \\ \alpha \cdot I_s + \beta, & I_s \geq I_m \end{cases}$	$\kappa = \alpha \cdot \exp(\beta \cdot I_s)$	$\kappa = \alpha \cdot I_s^\beta$

Table S3: Fitting parameters for Eq.7 (Main Manuscript) relating the relative image intensity I_s and the permeability κ .

	$d = 300 \mu\text{m}, Q = 1 \text{ mL/h}$	$d = 75 \mu\text{m}, Q = 1 \text{ mL/h}$	$d = 300 \mu\text{m}, Q = 0.2 \text{ mL/h}$
α	0.82	0.82	0.82
β	700	1700	300
γ	1	1	1